APL Materials

RESEARCH ARTICLE | JUNE 15 2023

Superconductivity at epitaxial $LaTiO_3$–$KTaO_3$ interfaces

D. Maryenko ; I. V. Maznichenko ; S. Ostanin ; M. Kawamura ; K. S. Takahashi ; M. Nakamura ; V. K. Dugaev ; E. Ya. Sherman ; A. Ernst ; M. Kawasaki

Check for updates

APL Mater 11, 061102 (2023)
https://doi.org/10.1063/5.0151227

View Online
Export Citation
CrossMark

07 August 2023 06:16:36

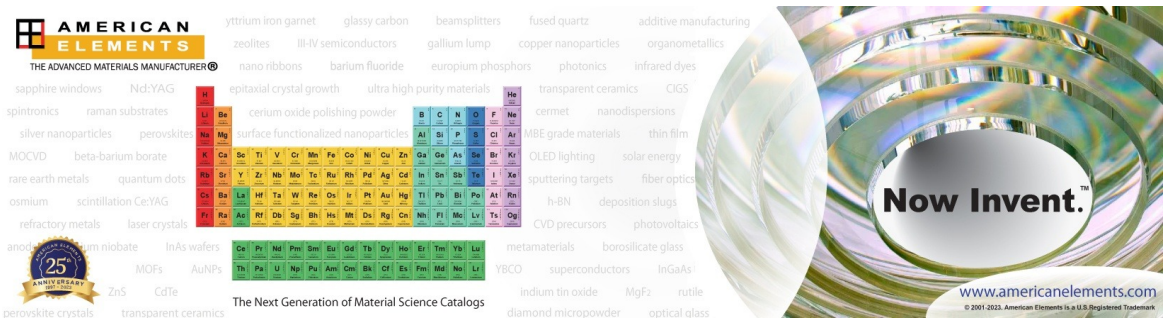

AIP Publishing

Superconductivity at epitaxial $LaTiO_3$–$KTaO_3$ interfaces

Cite as: APL Mater. 11, 061102 (2023); doi: 10.1063/5.0151227
Submitted: 20 March 2023 • Accepted: 9 May 2023 •
Published Online: 15 June 2023

View Online Export Citation CrossMark

D. Maryenko,[1,a)] I. V. Maznichenko,[2] S. Ostanin,[2] M. Kawamura,[1] K. S. Takahashi,[1] M. Nakamura,[1] V. K. Dugaev,[3] E. Ya. Sherman,[4,5] A. Ernst,[6,7] and M. Kawasaki[1,8]

AFFILIATIONS

[1] RIKEN Center for Emergent Matter Science (CEMS), Wako 351-0198, Japan
[2] Institute of Physics, Martin Luther University Halle-Wittenberg, 06120 Halle, Germany
[3] Department of Physics and Medical Engineering, Rzeszów University of Technology, 35-959 Rzeszów, Poland
[4] Department of Physical Chemistry and EHU Quantum Center, University of the Basque Country, 48940 Leioa, Spain
[5] Ikerbasque, Basque Foundation for Science, Bilbao, Spain
[6] Institute for Theoretical Physics, Johannes Kepler University, 4040 Linz, Austria
[7] Max Planck Institute of Microstructure Physics, D-06120 Halle, Germany
[8] Department of Applied Physics and Quantum-Phase Electronics Center (QPEC), The University of Tokyo, Tokyo 113-8656, Japan

[a)] **Author to whom correspondence should be addressed:** maryenko@riken.jp

07 August 2023 06:16:36

ABSTRACT

The design of epitaxial interfaces is a pivotal way to engineer artificial structures where new electronic phases can emerge. Here, we report a systematic emergence of an interfacial superconducting state in epitaxial heterostructures of $LaTiO_3$ and $KTaO_3$. The superconductivity transition temperature increases with decreasing thickness of $LaTiO_3$. Such a behavior is observed for both (110) and (111) crystal oriented structures. For thick samples, the finite resistance developing below the superconducting transition temperature increases with increasing $LaTiO_3$ thickness. Consistent with previous reports, the (001) oriented heterointerface features a high electron mobility of 250 $cm^2\ V^{-1}\ s^{-1}$ and shows no superconducting transition down to 40 mK. Our results imply a non-trivial impact of $LaTiO_3$ on the superconducting state and indicate how superconducting $KTaO_3$ interfaces can be integrated with other oxide materials.

© 2023 Author(s). All article content, except where otherwise noted, is licensed under a Creative Commons Attribution (CC BY) license (http://creativecommons.org/licenses/by/4.0/). https://doi.org/10.1063/5.0151227

I. INTRODUCTION

Interfaces between materials can harbor electronic structures distinct from the bulk constituents. One instance is the formation of a metallic layer at the junction of two insulators. A broadly celebrated example is the $LaAlO_3/SrTiO_3$ interface, which not only harbors high mobility carriers but can also become superconducting at around 300 mK.[1–3] This rather well controlled system became a fertile testbed to explore two-dimensional superconductivity. In such a strongly asymmetric heterostructure, it was straightforward to assay the role of spin–orbit coupling (SOC) for the superconducting phase, albeit the conduction band is formed by 3*d*-orbitals of titanium with a moderate SOC energy on the order of 40 meV.[4–7] In fact, it is anticipated that a sizable spin–orbit coupling can be favorable for unconventional Cooper pairing and for the realization of Majorana states.[8–12] Therefore, the recent observation of superconductivity in $KTaO_3$, whose conduction band is formed by 5*d* Ta orbitals with a much larger SOC energy of about 300 meV, may provide a new twist in the formation of the superconducting phase in two dimensions. Furthermore, by taking into consideration that bulk $KTaO_3$ has not still been demonstrated to become superconducting, the emergence of interfacial superconductivity in such a system can provide a distinct insight into the Cooper pair formation mechanism.[13] Being isostructural to $SrTiO_3$, the perovskite oxide $KTaO_3$ is a quantum paraelectric and has a bandgap of about 3.6 eV. The conduction band around Γ point is split by a large spin–orbit coupling in well separated bands with an effective

© Author(s) 2023

total angular momentum $J = 1/2$ (higher energy) and $J = 3/2$ states (lower energy).

The first observation of interfacial $KTaO_3$ superconductivity dates back to experiments with the ionic liquid gating technique, which has revealed a superconducting transition at 50 mK for (001)-oriented $KTaO_3$ surface.[14] Recently, the emergence of superconductivity at (110)- and (111)-oriented $KTaO_3$ surfaces was demonstrated in the majority of cases by growing a EuO layer or depositing an amorphous $LaAlO_3$ layer.[15–21] The cubic lattice structure of EuO with a lattice constant $a = 5.145$ Å matches neither (110) nor (111) orientation of the $KTaO_3$ crystal structure, resulting in the formation of either polycrystalline or defective layers at the interface.[16,17] Superconductivity was also observed in the (111)-oriented $KTaO_3$ heterostructure with a 10 nm thick $La_{2/3}Sr_{1/3}MnO_3$ top layer.[22] To have full control over the emergent superconducting state, it is important to have excellent control over the interface's electronic properties, which also includes the understanding of the role of the top layer in the emergent phenomena. This control paves the way for integrating superconducting $KTaO_3$ interfaces with other oxide materials.

Here, we report the emergence of superconductivity in the epitaxial-grown structures of $LaTiO_3$ on (110) and (111) oriented $KTaO_3$. We observe that the superconducting transition temperature increases with decreasing thickness of the $LaTiO_3$ layer. For thick samples, the resistance R_{xx} remains finite below the superconducting transition temperature and this R_{xx} value increases with increasing $LaTiO_3$ thickness. These observations indicate a nontrivial impact of $LaTiO_3$ on the interface's electronic properties. Our finding may facilitate the engineering of the superconducting phase at the interface. The bulk $LaTiO_3$ is a Mott insulator with an orthorhombic crystal structure and lattice parameters $a = b = 5.595$ Å and $c = 7.912$ Å. Therefore, $LaTiO_3$ can be thought of as a quasi-cubic structure with an effective lattice constant $\sqrt{a^2 + b^2}/2 \cong c/2 = 3.956$ Å, which, thus, differs by only about 0.8% from the lattice constant of cubic $KTaO_3$ $a = b = c = 3.989$ Å. This facilitates

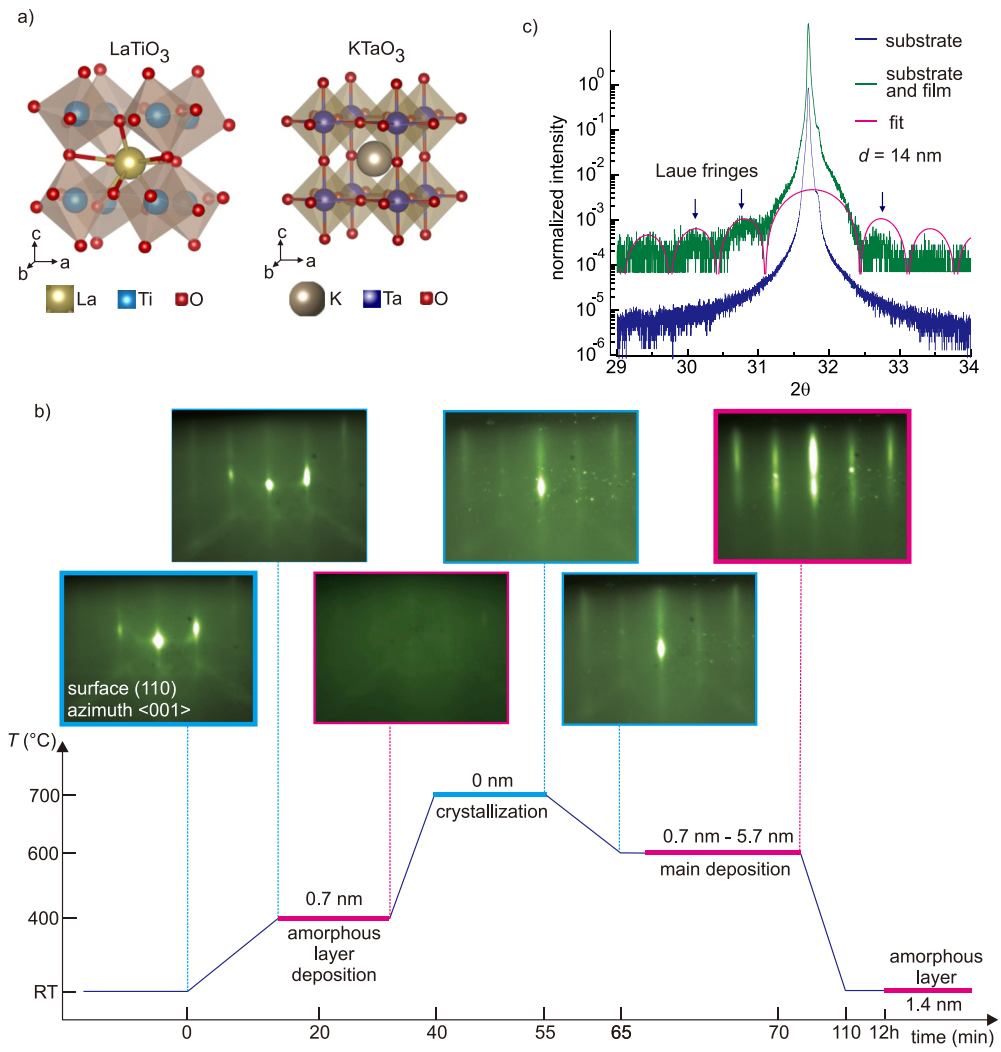

FIG. 1. (a) Crystal structure of $LaTiO_3$ and $KTaO_3$.[23] (b) Epitaxial growth process steps for $LaTiO_3/KTaO_3$ heterostructures. Shown are the RHEED patterns at various steps of the (110) oriented structure growth. A similar evolution of the RHEED pattern with temperature is also observed for structures grown on (001) and (111) $KTaO_3$ crystal orientations. (c) X-ray diffraction patterns of the (110)-oriented substrate (blue trace) and a film on a substrate (green trace). The diffraction pattern is shifted for clarity along the vertical axis. The red line is the best fit describing the position of Laue fringes.

07 August 2023 06:16:36

© Author(s) 2023

the growth of $LaTiO_3/KTaO_3$ heterostructures on the three main facets of a cubic crystal system, i.e., (001), (110), and (111).[24]

II. RESULTS AND DISCUSSION

A. Epitaxial growth

The $LaTiO_3/KTaO_3$ structures are grown using the pulsed laser deposition technique. A piece of the $KTaO_3$ substrate with a size of about 3 × 3 mm^2 was attached to the substrate holder using silver epoxy. A polycrystalline $La_2Ti_2O_7$ target is ablated in vacuum with a repetition rate of 2 Hz and a laser fluence of 1.6 J cm^{-2}. The growth chamber is equipped with a reflection high-energy electron diffraction (RHEED) monitor allowing us to observe the growth process *in situ*. Figure 1(b) shows the exemplary RHEED patterns during the growth process of the (110)-oriented structure. After loading the substrate in the growth chamber, the substrate is heated to 400 °C. During this heating step, no change in the RHEED pattern is observed. In fact, the atomic force microscopy measurements show that the surface morphology barely changes at 400 °C (see the supplementary material). To prevent the degradation of the $KTaO_3$ surface upon further heating and to suppress the formation of defects, the substrate surface is covered with an amorphous layer by ablating the $La_2Ti_2O_7$ target, which is indicated by the vanishing RHEED pattern after this processing step. Upon heating to 700 °C, the amorphous layer crystallizes and the streak pattern forms gradually. This solid state epitaxial step at 700 °C is favored due to a small lattice mismatch between $LaTiO_3$ and $KTaO_3$, which gives a clear diffraction pattern correspondence between the substrate and the crystallized layer. The crystallized layer enables successive homoepitaxial growth, which takes place at a lower temperature of 600 °C. The heterostructures discussed in this work differ by the $LaTiO_3$ layer thickness deposited at 600 °C. After the growth, the heterostructures are cooled to room temperature and are left to thermalize for about 12 h. Subsequently, the structures are covered with a thin amorphous layer by ablating the $La_2Ti_2O_7$ target to prevent potential degradation of structures under ambient conditions. We note that the growth conditions favor the stabilization of the $LaTiO_3$ phase.[25] To check the film crystal structure, we grow a thick $LaTiO_3$ layer with 735 pulses. Figure 1(c) shows its x-ray diffraction pattern (green trace) featuring Laue fringes, which indicate a high crystalline film quality. Due to the similar lattice parameters of $LaTiO_3$ and $KTaO_3$, the Bragg diffraction peak of $LaTiO_3$ is indiscernible due to the overlapped diffraction pattern of the substrate (blue trace). By fitting the position of the Laue fringes (red line), we determine a film thickness of 14 nm, which is used to estimate the thickness of thinner films from a given number of pulses as shown in Fig. 1(b) for each process step. The stoichiometry of the structures checked with energy-dispersive x-ray spectroscopy was comparable with that of the target. We note, however, that the exact stoichiometry of the structure can have an impact on the interface conductivity.[26–28]

B. Electrical transport characteristics

The transport characteristics of heterostructures are shown in Fig. 2. We employed a Physical Property Measurement System (PPMS, Quantum Design) down to 2 K and an adiabatic demagnetization refrigerator (ADR) stage, which is compatible with the PPMS platform, to characterize the superconducting transition of heterostructures down to 150 mK. The samples are directly bonded with aluminum wires as shown in Fig. 3(a) so that they can be characterized along two orthogonal directions simultaneously. Figures 2(a) and 2(b) show the exemplary temperature dependence of R_{xx} for three crystal orientations. Consistent with previous reports, the (111)-oriented heterostructure has a higher superconducting transition temperature than the (110)-oriented heterostructures.[15–17,19] More importantly, we observe that the onset temperature of the superconducting phase T_c^{onset} strongly depends on the thickness of the $LaTiO_3$ layer. Such an impact of the top layer thickness on the superconducting state has not been reported yet. Figure 2(c) shows that T_c^{onset} increases with decreasing thickness of the $LaTiO_3$ layer. Such a behavior is observed for both (110) and (111) oriented heterostructures. Following this finding, we measured one of the (001)-oriented heterostructures with a 1.7 nm thick $LaTiO_3$ layer in a dilution refrigerator at a temperature down to 40 mK but did not observe a superconducting transition. The absence of a superconducting phase for (001) oriented heterostructures is consistent with a previous report.[19] To check the conductance of the $LaTiO_3$ layer, we grew a 2.6 nm thin $LaTiO_3$ layer on both $GdScO_3$ and $NdScO_3$ substrates according to the growth procedure of Fig. 1. The

07 August 2023 06:16:36

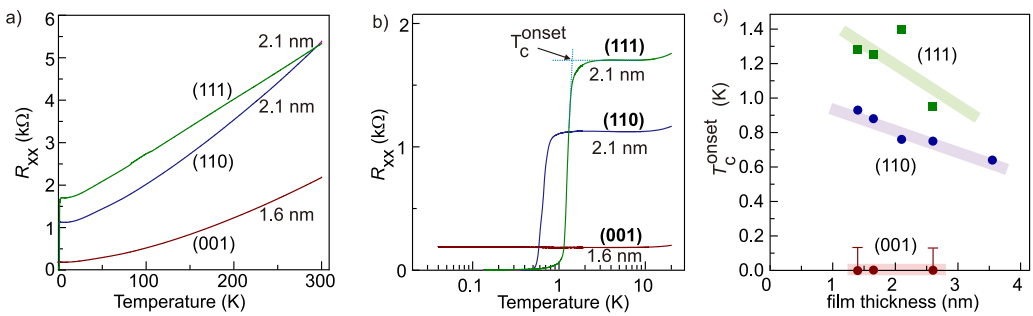

FIG. 2. (a) Exemplary temperature dependence of resistance for $LaTiO_3/KTaO_3$ heterostructures defined on (001), (110), and (111) crystal surfaces. (b) Superconducting state is observed for (110) and (111) oriented heterostructures, while (001) structure remains metallic down to 40 mK. Shown is the definition of the superconductivity onset temperature T_c^{onset}. (c) T_c^{onset} decreases with increasing thickness of $LaTiO_3$. We assign an error bar of 150 mK for (001)-oriented heterostructures, which are not measured in a dilution refrigerator. The thick lines are a guide to the eye.

© Author(s) 2023

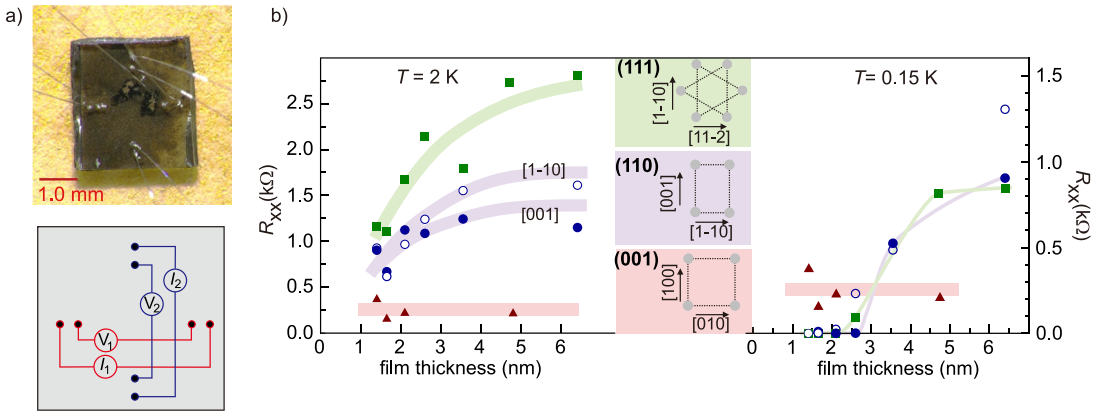

FIG. 3. (a) Photograph of a sample with attached wires to measure the temperature dependence of sample resistance. Also shown is the scheme of the electrical circuit sample connection. A multi-channel source-measurement unit of the PPMS is used to measure two orthogonal crystal directions simultaneously. (b) Resistance at zero magnetic field at T = 2 K (above superconducting transition, left panel) and at T = 150 mK (below superconducting transition, right panel) as a function of the $LaTiO_3$ thickness. The color encodes the crystal orientation of heterostructures. The thin heterostructures with (110) and (111) crystal orientations show R_{xx} = 0 Ω at T = 150 mK. As the $LaTiO_3$ thickness increases, the residual R_{xx} increases. The thick lines are a guide to the eye.

resistance of such structures at room temperature was on the order of 10^6 Ω.

Figure 3(b) compares the resistance values of heterostructures above (T = 2 K, left panel) and below (T = 150 mK, right panel) the superconducting transition. It is noticeable that R_{xx} at T = 2 K increases with increasing $LaTiO_3$ thickness for both the (111) and (110) oriented structures, while it remains almost constant for the (001)-oriented heterostructures. Such a behavior points to the interface conductance rather than to the conductance in the $LaTiO_3$ layer solely, in which case the resistance would decrease with increasing $LaTiO_3$ thickness. To further elucidate the properties of the heterostructures, we show in Fig. 4 the dependence of both the electron mobility and the charge carrier density on the $LaTiO_3$ thickness. The charge carrier density n is estimated from the Hall effect measurements, while mobility μ is estimated from the sample conductance in a zero magnetic field. Among the three crystal orientations, the (001)-oriented heterointerface has the highest electron mobility on the order of 250 $cm^2\ V^{-1}\ s^{-1}$, which does not depend on the $LaTiO_3$ thickness. Both the electron mobility and the charge carrier density values are consistent with those obtained for $LaTiO_3/KTaO_3$ (001)-oriented structures grown by molecular beam epitaxy.[24] For both the (110) and (111) oriented heterostructures, the electron mobility shows a distinct behavior; it is the largest for thin structures, i.e., around 100 $cm^2\ V^{-1}\ s^{-1}$, and decreases with increasing $LaTiO_3$ thickness, reaching a saturation value of around 30 $cm^2\ V^{-1}\ s^{-1}$ above a $LaTiO_3$ thickness of 2 nm. By contrast, the charge carrier density shows a fast increase with the $LaTiO_3$ thickness by about a factor of 1.5 (lower panel in Fig. 4) and saturates above 2 nm. This seems to be a common tendency for all three crystal orientations. An increase in the sheet charge carrier density n [Fig. 4(b)] and, at the same time, a decrease in T_c^{onset} with the $LaTiO_3$ thickness [Fig. 2(c)] establishes an opposite tendency to the previous observations in $KTaO_3$-based superconducting structures, for which the superconducting transition temperature increases with increasing n.[19,20] The presented results indicate an impact of the epitaxial $LaTiO_3$ layer on the electronic properties of the interface, which also affects the superconducting regime as we discuss now.

The right panel in Fig. 3(b) shows the dependence of R_{xx} at 150 mK (well below T_c^{onset}) on the $LaTiO_3$ thickness for all heterostructures. For the sake of comparison, it also contains data

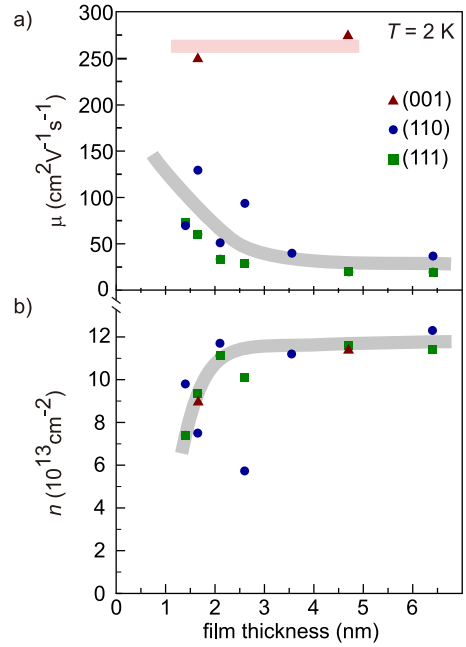

FIG. 4. Mobility (a) and charge carrier density (b) dependence on the $LaTiO_3$ layer thickness at T = 2 K for different heterostructure orientations. The charger carrier density is estimated from the transverse resistance R_{xy} (Hall effect), which changes linearly with the magnetic field B. The thick lines are a guide to the eye.

07 August 2023 06:16:36

© Author(s) 2023

points for the high mobility (001) interface that does not become superconducting in our experiments. A well-developed superconducting state characterized by $R_{xx} = 0\ \Omega$ is reached for both (110)- and (111)-oriented heterostructures but only with a thin $LaTiO_3$ layer. For thicker $LaTiO_3$ layers, R_{xx} attains a non-zero value, which increases with increasing $LaTiO_3$ thickness. Furthermore, we detect an anisotropy for the (110)-oriented structures. The open symbols in the right panel depict the R_{xx} values measured along the [1-10] direction at 150 mK. For 2.1 and 2.6 nm thick samples, the superconductivity along the [001] direction survives at 150 mK, while R_{xx} along the [1-10] direction has a non-zero value. (In the supplementary material, we show the temperature dependence of R_{xx} during the superconducting transition for all samples.) By contrast to (110)-oriented structures, [1-10] and [11-2] crystal directions of (111)-oriented heterostructures appear to be equivalent. Since the heterostructures are grown in equivalent procedures, it allows us to conclude that a potential sample inhomogeneity cannot explain the anisotropy as observed in (110)-oriented structures. This surprising emergence of the anisotropic behavior of R_{xx} below the superconducting transition is perhaps related to the immanent electronic structure of the interface. Anisotropy for (110)-oriented heterostructures is reported for the normal conducting state of $SrTiO_3$-based heterostructures and is related to a different arrangement of interface atoms along the [001] and [1-10] directions.[29,30] An indication of such an anisotropy in our (110)-oriented heterostructures might also appear in the normal conducting state. At $T = 2$ K, Fig. 3(b) (left panel) depicts that R_{xx} along the [1-10] direction (open blue symbols) is larger than that along the [001] direction (full blue symbols).

Beyond that, increasing the $LaTiO_3$ thickness affects the transport characteristics of both the (110)- and (111)-oriented heterostructures before the superconducting transition. In fact, for structures with a thicker $LaTiO_3$, one clearly observes some increase in $R_{xx} \propto \ln T$, indicating a contribution of the weak localization correction to the sample resistance (see the supplementary material). This has also been observed in superconducting $LaTiO_3/SrTiO_3$ structures.[31] Conspicuously, when this localization behavior is strongly pronounced in our structures, $R_{xx} = 0\ \Omega$ vanishes for (110) as well as for (111)-oriented structures, as shown in the supplementary material. The (110) and (111) heterostructures feature a weak antilocalization behavior in magnetotransport, indicating a significance of spin–orbit coupling. Intriguingly, weak antilocalization is barely pronounced for non-superconducting (001)-oriented heterostructures (see the supplementary material).

The observation of the superconducting transition being dependent on the $KTaO_3$ surface orientation is consistent with previous reports on superconductivity in $KTaO_3$.[15–19] This allows us to conclude that the superconducting phase in our structures involves the electronic states of $KTaO_3$. At the same time, the $LaTiO_3$ thickness dependence of the transport characteristics in both superconducting and normal states implies a non-trivial impact of the top layer on the electronic structure of the $LaTiO_3/KTaO_3$ heterointerface. In the vicinity of the junction, the Ta atoms are in a 5+ state, whereas Ti is in a 3+ state. This charge discontinuity can lead to charge redistribution between the $LaTiO_3$ and $KTaO_3$ layers adjacent to the interface, creating an interfacial conducting layer. One such mechanism can be related to the so-called polar catastrophe, which is based on the compensation of the diverging electrostatic energy at the interface.[32] This mechanism has been considered for various $SrTiO_3$ and $KTaO_3$ based heterostructures and can be effective for (001) and (111) oriented structures but is not obvious for (110) structures.[24,33–36] Surface reconstruction and the modification of TiO_6 octahedra have also been considered for the emergence of conducting layers at the interface between band insulators and Mott insulators, such as $LaTiO_3$.[37–39] Moreover, oxygen defects can contribute to the emergence of a conducting layer. It would require additional experimental and theoretical efforts to elucidate how each of those mechanisms is realized in our superconducting $LaTiO_3/KTaO_3$ structures. The interplay of those mechanisms will define the extension of the conducting layer, the interaction between the $LaTiO_3$ and $KTaO_3$ layers, and, consequently the total electronic structure.

III. CONCLUSION

In summary, we have grown epitaxial $LaTiO_3/KTaO_3$ heterostructures with (001), (110), and (111) crystal orientations and varying the $LaTiO_3$ thickness. The (110)- and (111)-oriented heterostructures have a moderate electron mobility and a well-developed superconducting state. The (001)-oriented heterostructures have the highest electron mobility with no indication of a superconducting transition. The $LaTiO_3$ layer has a non-trivial impact on the emergence of the superconducting phase. With increasing $LaTiO_3$ thickness, the superconducting transition temperature decreases and a finite resistance remains below the transition. This behavior seems to correlate with the emergence of electron weak localization. Furthermore, for the (110)-oriented heterostructures, we observe a regime when $R_{xx} = 0\ \Omega$ along the [001] direction and non-zero for the [1-10] direction, thus establishing anisotropic superconductivity in the $LaTiO_3/KTaO_3$-heterostructures. Our result may pave the way for engineering superconducting interfaces and integrating superconducting $KTaO_3$ interfaces with oxide materials.

SUPPLEMENTARY MATERIAL

See the supplementary material for additional details on superconducting transition, features of weak antilocalization behavior in the magnetic field, and atomic force microscopy images.

ACKNOWLEDGMENTS

We thank Dr. M. Kriener and Dr. M. Birch for the fruitful discussion and careful reading of the manuscript. This work was supported by JSPS KAKENHI (Grant No. 22H04958). The work of E.Y.S. was supported through Grant Nos. PGC2018-101355-B-I00 and PID2021-126273NB-I00 funded by Grant No. MCIN/AEI/10.13039/501100011033 and by the ERDF "A way of making Europe," and by the Basque Government through Grant No. IT1470-22. The work of V.K.D. was supported by the National Science Center in Poland as a research project under Grant No. DEC-2017/27/B/ST3/02881.

07 August 2023 06:16:36

© Author(s) 2023

AUTHOR DECLARATIONS

Conflict of Interest

The authors have no conflicts to disclose.

Author Contributions

D. Maryenko: Conceptualization (lead); Formal analysis (lead); Investigation (lead); Methodology (lead); Writing – original draft (lead); Writing – review & editing (lead). **I. V. Maznichenko**: Investigation (equal); Writing – review & editing (equal). **S. Ostanin**: Investigation (equal); Writing – review & editing (equal). **M. Kawamura**: Investigation (supporting); Writing – review & editing (equal). **K. S. Takahashi**: Investigation (supporting); Writing – review & editing (equal). **M. Nakamura**: Investigation (supporting); Writing – review & editing (equal). **V. K. Dugaev**: Funding acquisition (equal); Investigation (equal); Writing – review & editing (equal). **E. Ya. Sherman**: Funding acquisition (equal); Investigation (equal); Writing – review & editing (equal). **A. Ernst**: Funding acquisition (equal); Investigation (equal); Writing – review & editing (equal). **M. Kawasaki**: Formal analysis (equal); Funding acquisition (lead); Writing – original draft (equal); Writing – review & editing (equal).

DATA AVAILABILITY

The data that support the findings of this study are available from the corresponding author upon reasonable request.

REFERENCES

[1] A. Ohtomo and H. Y. Hwang, "A high-mobility electron gas at the $LaAlO_3/SrTiO_3$ heterointerface," Nature **427**, 423–426 (2004).

[2] N. Reyren, S. Thiel, A. D. Caviglia, L. F. Kourkoutis, G. Hammerl, C. Richter, C. W. Schneider, T. Kopp, A.-S. Rüetschi, D. Jaccard, M. Gabay, D. A. Muller, J.-M. Triscone, and J. Mannhart, "Superconducting interfaces between insulating oxides," Science **317**, 1196–1199 (2007).

[3] A. D. Caviglia, S. Gariglio, N. Reyren, D. Jaccard, T. Schneider, M. Gabay, S. Thiel, G. Hammerl, J. Mannhart, and J.-M. Triscone, "Electric field control of the $LaAlO_3/SrTiO_3$ interface ground state," Nature **456**, 624–627 (2008).

[4] Y. A. Bychkov and E. I. Rashba, "Properties of a 2D electron gas with lifted spectral degeneracy," JETP Lett. **39**, 78–81 (1984).

[5] A. D. Caviglia, M. Gabay, S. Gariglio, N. Reyren, C. Cancellieri, and J.-M. Triscone, "Tunable Rashba spin-orbit interaction at oxide interfaces," Phys. Rev. Lett. **104**, 126803 (2010).

[6] M. Ben Shalom, M. Sachs, D. Rakhmilevitch, A. Palevski, and Y. Dagan, "Tuning spin-orbit coupling and superconductivity at the $SrTiO_3/LaAlO_3$ interface: A magnetotransport study," Phys. Rev. Lett. **104**, 126802 (2010).

[7] G. Herranz, G. Singh, N. Bergeal, A. Jouan, J. Lesueur, J. Gázquez, M. Varela, M. Scigaj, N. Dix, F. Sánchez, and J. Fontcuberta, "Engineering two-dimensional superconductivity and Rashba spin–orbit coupling in $LaAlO_3/SrTiO_3$ quantum wells by selective orbital occupancy," Nat. Commun. **6**, 6028 (2015).

[8] J. W. F. Venderbos, L. Savary, J. Ruhman, P. A. Lee, and L. Fu, "Pairing states of spin-$\frac{3}{2}$ fermions: Symmetry-enforced topological gap functions," Phys. Rev. X **8**, 011029 (2018).

[9] L. P. Gor'kov and E. I. Rashba, "Superconducting 2D system with lifted spin degeneracy: Mixed singlet-triplet state," Phys. Rev. Lett. **87**, 037004 (2001).

[10] M. S. Scheurer and J. Schmalian, "Topological superconductivity and unconventional pairing in oxide interfaces," Nat. Commun. **6**, 6005 (2014).

[11] V. Kozii and L. Fu, "Odd-parity superconductivity in the vicinity of inversion symmetry breaking in spin-orbit-coupled systems," Phys. Rev. Lett. **115**, 207002 (2015).

[12] S. Nakosai, Y. Tanaka, and N. Nagaosa, "Topological superconductivity in bilayer Rashba system," Phys. Rev. Lett. **108**, 147003 (2012).

[13] S. H. Wemple, "Some transport properties of oxygen-deficient single-crystal potassium tantalate $KTaO_3$," Phys. Rev. **137**, A1575–A1582 (1965).

[14] K. Ueno, S. Nakamura, H. Shimotani, H. T. Yuan, N. Kimura, T. Nojima, H. Aoki, Y. Iwasa, and M. Kawasaki, "Discovery of superconductivity in $KTaO_3$ by electrostatic carrier doping," Nat. Nanotechnol. **6**, 408–412 (2011).

[15] Z. Chen, Z. Liu, Y. Sun, X. Chen, Y. Liu, H. Zhang, H. Li, M. Zhang, S. Hong, T. Ren, C. Zhang, H. Tian, Y. Zhou, J. Sun, and Y. Xie, "Two-dimensional superconductivity at the $LaAlO_3/KTaO_3(110)$ heterointerface," Phys. Rev. Lett. **126**, 026802 (2021).

[16] C. Liu, X. Yan, D. Jin, Y. Ma, H.-W. Hsiao, Y. Lin, T. M. Bretz-Sullivan, X. Zhou, J. Pearson, B. Fisher, J. S. Jiang, W. Han, J.-M. Zuo, J. Wen, D. D. Fong, J. Sun, H. Zhou, and A. Bhattacharya, "Two-dimensional superconductivity and anisotropic transport at $KTaO_3(111)$ interfaces," Science **371**, 716–721 (2021).

[17] X. Hua, F. Meng, Z. Huang, Z. Li, S. Wang, B. Ge, Z. Xiang, and X. Chen, "Tunable two-dimensional superconductivity and spin-orbit coupling at the $EuO/KTaO_3(110)$," npj Quantum Mater. **7**, 97 (2022).

[18] Z. Chen, Y. Liu, H. Zhang, Z. Liu, H. Tian, Y. Sun, M. Zhang, Y. Zhou, J. Sun, and Y. Xie, "Electric field control of superconductivity at the $LaAlO_3/KTaO_3(111)$ interface," Science **372**, 721–724 (2021).

[19] C. Liu, X. Zhou, D. Hong, B. Fisher, H. Zheng, J. Pearson, J. S. Jiang, D. Jin, M. R. Norman, and A. Bhattacharya, "Tunable superconductivity and its origin at $KTaO_3$ interfaces," Nat. Commun. **14**, 951 (2023).

[20] S. Mallik, G. C. Ménard, G. Saïz, H. Witt, J. Lesueur, A. Gloter, L. Benfatto, M. Bibes, and N. Bergeal, "Superfluid stiffness of a $KTaO_3$-based two-dimensional electron gas," Nat. Commun. **13**, 4625 (2022).

[21] A. H. Al-Tawhid, J. Kanter, M. Hatefipour, D. P. Kumah, J. Shabani, and K. Ahadi, "Superconductivity and weak antilocalization at $KTaO_3(111)$ interfaces," J. Electron. Mater. **51**, 6305 (2022).

[22] E. G. Arnault, A. H. Al-Tawhid, S. Salmani-Rezaie, D. A. Muller, D. P. Kumah, M. S. Bahramy, G. Finkelstein, and K. Ahadi, "Anisotropic superconductivity at $KTaO_3(111)$ interfaces," Sci. Adv. **9**, eadf1414 (2023).

[23] K. Momma and F. Izumi, "VESTA 3 for three-dimensional visualization of crystal, volumetric and morphology data," J. Appl. Crystallogr. **44**, 1272–1276 (2011).

[24] K. Zou, S. Ismail-Beigi, K. Kisslinger, X. Shen, D. Su, F. J. Walker, and C. H. Ahn, "$LaTiO_3/KTaO_3$ interfaces: A new two-dimensional electron gas system," APL Mater. **3**, 036104 (2015).

[25] A. Ohtomo, D. A. Muller, J. L. Grazul, and H. Y. Hwang, "Epitaxial growth and electronic structure of $LaTiO_x$ films," Appl. Phys. Lett. **80**, 3922–3924 (2002).

[26] E. Breckenfeld, N. Bronn, J. Karthik, A. R. Damodaran, S. Lee, N. Mason, and L. W. Martin, "Effect of growth induced (non)stoichiometry on interfacial conductance in $LaAlO_3/SrTiO_3$," Phys. Rev. Lett. **110**, 196804 (2013).

[27] H. K. Sato, C. Bell, Y. Hikita, and H. Y. Hwang, "Stoichiometry control of the electronic properties of the $LaAlO_3/SrTiO_3$ heterointerface," Appl. Phys. Lett. **102**, 251602 (2013).

[28] M. P. Warusawithana, C. Richter, J. A. Mundy, P. Roy, J. Ludwig, S. Paetel, T. Heeg, A. A. Pawlicki, L. F. Kourkoutis, M. Zheng, M. Lee, B. Mulcahy, W. Zander, Y. Zhu, J. Schubert, J. N. Eckstein, D. A. Muller, C. S. Hellberg, J. Mannhart, and D. G. Schlom, "$LaAlO_3$ stoichiometry is key to electron liquid formation at $LaAlO_3/SrTiO_3$ interfaces," Nat. Commun. **4**, 2351 (2013).

[29] A. Annadi, Q. Zhang, X. Renshaw Wang, N. Tuzla, K. Gopinadhan, W. M. Lü, A. Roy Barman, Z. Q. Liu, A. Srivastava, S. Saha, Y. L. Zhao, S. W. Zeng, S. Dhar, E. Olsson, B. Gu, S. Yunoki, S. Maekawa, H. Hilgenkamp, T. Venkatesan, and Ariando, "Anisotropic two-dimensional electron gas at the $LaAlO_3/SrTiO_3(110)$ interface," Nat. Commun. **4**, 1838 (2013).

[30] Z. Wang, Z. Zhong, X. Hao, S. Gerhold, B. Stöger, M. Schmid, J. Sánchez-Barriga, A. Varykhalov, C. Franchini, K. Held, and U. Diebold, "Anisotropic two-dimensional electron gas at $SrTiO_3(110)$," Proc. Natl. Acad. Sci. U. S. A. **111**, 3933–3937 (2014).

[31] J. Biscaras, N. Bergeal, A. Kushwaha, T. Wolf, A. Rastogi, R. C. Budhani, and J. Lesueur, "Two-dimensional superconductivity at a Mott insulator/band insulator interface $LaTiO_3/SrTiO_3$," Nat. Commun. **1**, 89 (2010).

07 August 2023 06:16:36

© Author(s) 2023

[32]N. Nakagawa, H. Y. Hwang, and D. A. Muller, "Why some interfaces cannot be sharp," Nat. Mater. **5**, 204–209 (2006).
[33]A. Ohtomo, D. A. Muller, J. L. Grazul, and H. Y. Hwang, "Artificial charge-modulation in atomic-scale perovskite titanate superlattices," Nature **419**, 378–380 (2002).
[34]Y. Hotta, T. Susaki, and H. Y. Hwang, "Polar discontinuity doping of the $LaVO_3/SrTiO_3$ interface," Phys. Rev. Lett. **99**, 236805 (2007).
[35]P. Moetakef, T. A. Cain, D. G. Ouellette, J. Y. Zhang, D. O. Klenov, A. Janotti, C. G. Van de Walle, S. Rajan, S. J. Allen, and S. Stemmer, "Electrostatic carrier doping of $GdTiO_3/SrTiO_3$ interfaces," Appl. Phys. Lett. **99**, 232116 (2011).
[36]A. H. Al-Tawhid, D. P. Kumah, and K. Ahadi, "Two-dimensional electron systems and interfacial coupling in $LaCrO_3/KTaO_3$ heterostructures," Appl. Phys. Lett. **118**, 192905 (2021).
[37]S. Okamoto and A. J. Millis, "Electronic reconstruction at an interface between a Mott insulator and a band insulator," Nature **428**, 630 (2004).
[38]S. Okamoto, A. J. Millis, and N. A. Spaldin, "Lattice relaxation in oxide heterostructures: $LaTiO_3/SrTiO_3$ superlattices," Phys. Rev. Lett. **97**, 056802 (2006).
[39]H. Ishida and A. Liebsch, "Origin of metallicity of $LaTiO_3/SrTiO_3$ heterostructures," Phys. Rev. B **77**, 115350 (2008).

07 August 2023 06:16:36

© Author(s) 2023